Vilnius University
Institute of Mathematics and Informatics
L I T H U A N I A

INFORMATICS (09 P)

NUMERICAL AND SYMBOLIC MODELING OF REACTION-DIFFUSION PROCESSES IN BIOREACTORS

Linas Petkevičius

October 2018

Technical Report MII-DS-09P-18-16

VU Institute of Mathematics and Informatics, Akademijos str. 4, Vilnius LT-08663, Lithuania
www.mii.lt

Abstract

Microbioreactors are widely used in diagnostic and analytical systems, in the chemical industry, in the cleaning of contaminated fluids, in healthcare products, in the development of medicines. Microbiological reactors use very small amounts of catalysts and other materials, which greatly reduces production and analysis costs, shortens the process time, and makes the systems more compact. The relatively high cost of designing and optimizing new bioprocesses and microbioresactors can be greatly reduced by using mathematical and computer tools that often allow you to look at complicated processes, internal behavior. In the reporting year, the properties of microbioreactors in closed and open systems were investigated, a mathematical and computer model was developed [5,6,35,36]. In the coming years, microbioreactors of complex processes will be modeled, and the model will be validated by experimental data. These scientific results will help to create microreactors more efficiently at the design stage.

Keywords: reaction-diffusion, Michaelis - Menten kinetics, microbioreactor

Contents

1 Introduction

Batch stirred tank reactors (BSTR) are common in chemical industries [1,8,33]. Although a stirred tank is a common construction of industrial enzyme reactors, the effectiveness and optimal construction of RSTR remain open to study [17]. Recently a lot studies investigated BSTR type systems modeling [37], especelly investigation the effectiveness [10–12] of bioreactors.

In the last few decades, immobilized enzyme reactor models have evolved significantly with wide range of applications in food industry [21], waste cleaning [45], bacteria cells immobilization [15, 30]. It's become more usual to use immobilized enzyme porous microbioreactors as catalyst in BSTR [9, 11]. Similiar approach is also used in continuous stirred tank reactors (CSTR) [6, 20, 32, 42]. Differently from CSTR is that batch mode is closed system, so no new substrate appear in reactor at any point in reaction time, so hole system is more simple.

Mathematical models have been widely used to investigate the kinetic peculiarities of the enzyme microreactors [28, 42]. Models coupling the enzyme-catalysed reaction with the diffusion in enzyme microreactors are usually used. Since containing catalytic particles, the analyte in RSTR is well stirred and set in powerful motion, the mass transport by diffusion outside the microreactors is usually neglected [29, 34]. In practice, the zero thickness of the diffusion shell can not be achieved [44]. We consider an array of identical spherical microreactors placed in a RSTR shown in Figure 1 [20], where area Ω_m denotes a microreactor, Ω_d denotes surrounding diffusion shell and Ω_c is a convective region.

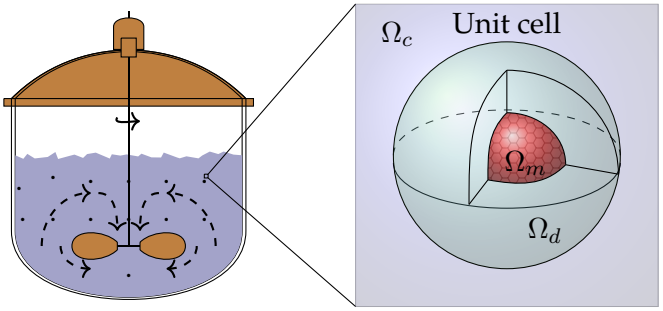

Figure 1: Batch stirred tank reactor with enzyme-loaded microreactors (pellets) and a zoomed unit cell to be modelled.

The limiting values of BSTR are simple: reactions reach quazi-steady-state and concentrations approach to zero, while transient effectiveness factor approach to limiting values [11]. However, the time until the quazi-steady-state is reached, or amount of product is produced in fixed time vary a lot. Dependent on initial conditions in this case whether microreactors are placed or injected into tank reactor, time might vary by magnitude of order.

The goal of this work was to investigate the different injection modes influence on process duration, as well as transient effectiveness factor. System is modeled by

reaction-diffusion equations, containing a non-linear term related to Michaelis-Menten kinetics [4, 20, 42]. The computer simulation was carried out using the finite difference technique [14].

The rest of the paper is organised as follows: in Section 2, the mathematical model and microbioreactor characteristics are described; Section 3 formulates a dimensionless model and derives the main parameters of the bioreactor; Section 4 describes the numerical model and the simulator; in Section 5, results of numerical experiments are presented, and conclusions close the article.

2 Mathematical model

We consider an array of identical spherical microreactors (MR) placed in a batch ideally stirred-tank reactor [11, 20]. Assuming a uniform distribution of the microreactors in the tank and a relatively great distance between adjacent microreactors, the spherical unit cell was modelled by an enzyme-loaded microreactor (pellet) and a surrounding diffusion shell (the Nernst layer). The principal structure of the tank containing uniformly distributed microreactors and a unit cell are presented in Figure 1.

In the enzyme-loaded MR layer we consider the enzyme-catalyzed reaction

$$\mathrm{E} + \mathrm{S} \underset{k_r}{\overset{k_f}{\rightleftharpoons}} \mathrm{ES} \xrightarrow{k_{\mathrm{cat}}} \mathrm{E} + \mathrm{P}, \tag{1}$$

where the substrate (S) combines reversibly with an enzyme (E) to form a complex (ES). The complex then dissociates into the product (P) and the enzyme is regenerated [16, 25]. The k_f, k_r and k_{cat} are forward rate, reverse rate and catalytic rate constanst, respectively.

Assuming the steady-state approximation, the concentration of the intermediate complex (ES) does not change and may be neglected when modelling the biochemical behaviour of the microreactor [20, 25, 39]. In the resulting scheme, the substrate (S) is enzymatically converted to the product (P),

$$\mathrm{S} \xrightarrow{\mathrm{E}} \mathrm{P}. \tag{2}$$

2.1 Governing Equations

Assuming the symmetrical spherical geometry of the microbioreactor and homogenised distribution of the immobilized enzyme inside the porous microreactor, the mathematical model can be described in one-dimensional domain using the radial distance [3].

Coupling enzymatic reaction in the microreactor (region Ω_m) with the one-dimensional-in-space diffusion, described by Fick's second law, lead to the following

governing equations of the reaction-diffusion type ($0 < \rho < \rho_0$):

$$\frac{\partial S_m}{\partial t} = \mathrm{D}_{S,m}\frac{1}{\rho^2}\frac{\partial}{\partial \rho}\Big(\rho^2\frac{\partial S_m}{\partial \rho}\Big) - \frac{\mathrm{V}_{\max} S_m}{\mathrm{K_M} + S_m}, \tag{3a}$$

$$\frac{\partial P_m}{\partial t} = \mathrm{D}_{P,m}\frac{1}{\rho^2}\frac{\partial}{\partial \rho}\Big(\rho^2\frac{\partial P_m}{\partial \rho}\Big) + \frac{\mathrm{V}_{\max} S_m}{\mathrm{K_M} + S_m}, \tag{3b}$$

where ρ stands for spherical space, $S_m = S_m(\rho,\ t)$ and $P_m = P_m(\rho,\ t)$ are the concentrations of the substrate and the reaction product in the microreactor, respectively, ρ_0 is the radius of the microreactor, $\mathrm{D}_{S,m}$ and $\mathrm{D}_{P,m}$ are the diffusion coefficients, $\mathrm{V}_{\max} = \mathrm{k_{cat}E_0}$ is the maximal enzymatic rate and $\mathrm{K_M} = (\mathrm{k_r} + \mathrm{k_{cat}})/\mathrm{k_f}$ is the Michaelis constant.

In the Nernst diffusion layer Ω_d only the mass transport by diffusion takes place $\rho \in (\rho_0,\ \rho_1)$:

$$\frac{\partial S_d}{\partial t} = \mathrm{D}_{S,d}\frac{1}{\rho^2}\frac{\partial}{\partial \rho}\Big(\rho^2\frac{\partial S_d}{\partial \rho}\Big), \tag{4a}$$

$$\frac{\partial S_d}{\partial t} = \mathrm{D}_{P,d}\frac{1}{\rho^2}\frac{\partial}{\partial \rho}\Big(\rho^2\frac{\partial P_d}{\partial \rho}\Big),$$

where $S_d = S_d(\rho,\ t)$ and $P_d = P_d(\rho,\ t)$ are the concentrations of the substrate and the reaction product in the diffusion shell, respectively, $\mathrm{D}_{S,d}$ and $\mathrm{D}_{P,d}$ are the diffusion coefficients of the materials in the bulk solution, ρ_1 is the radius of the unit cell. The thickness of the convective shell $\nu_1 = \rho_1 - \rho_0$ of the diffusion shell depends upon mixing speed in the buffer solution. The more intense stirring corresponds to the thinner diffusion shell (greater ν_1) [42] [7].

The intensive mixing of the solution and assumption that substrate is uniformly distributed throughout the outside of the diffusion shell implies that concentration depends only on time [19]. The rate at which substrate leaves the convective enclosure of volume $4/3\pi\rho_2^3 - 4/3\pi\rho_1^3$ is always to be equal to that at which it enters the diffusion shell over the surface of the area $4\pi\rho_1^2$, $\quad t > 0$,

$$\frac{\mathrm{d}S_b}{\mathrm{d}t} = \frac{1}{q}\mathrm{D}_{S,b}\frac{\partial S_d}{\partial \rho}\Big|_{\rho_1}, \tag{5a}$$

$$\frac{\mathrm{d}P_b}{\mathrm{d}t} = \frac{1}{q}\mathrm{D}_{S,b}\frac{\partial P_d}{\partial \rho}\Big|_{\rho_1}, \tag{5b}$$

where $S_b = S_b(t)$, $P_b = P_b(t)$ is the substrate and product concentrations in the bulk, ρ_2 is the radius of bulk, q is the ratio of the volume of the convective enclosure to the area of the outer surface of the diffusion shell $\rho = \rho_1$:

$$q = \frac{4\pi(\rho_2^3 - \rho_1^3)/3}{4\pi\rho_1^2} = \frac{\rho_2^3 - \rho_1^3}{3\rho_1^2}. \tag{6}$$

The value $1/q$ can be also considered as the adsorption capacity of the MR [9].

2.2 Boundary Conditions

Fluxes of the substrate and the product through the stagnant external diffusion shell is assumed to be equal to the corresponding fluxes entering the surface of the microreactor $t > 0$,

$$\mathrm{D}_{S,m}\frac{\partial S_m}{\partial \rho}\Big|_{\rho=\rho_0} = \mathrm{D}_{S,d}\frac{\partial S_d}{\partial \rho}\Big|_{\rho=\rho_0}, \tag{7a}$$

$$\mathrm{D}_{P,m}\frac{\partial P_m}{\partial \rho}\Big|_{\rho=\rho_0} = \mathrm{D}_{P,d}\frac{\partial P_d}{\partial \rho}\Big|_{\rho=\rho_0}. \tag{7b}$$

The formal partition coefficient ϕ is used to describe the specificity in concentration distribution of the compounds between two neighboring regions [20, 41] $t > 0$,

$$S_m(\rho_0) = \phi S_d(\rho_0), \;\; P_m(\rho_0) = \phi P_d(\rho_0). \tag{8}$$

Due to the symmetry of the microreactor, the zero-flux boundary conditions are defined for the center of the microreactor ($\rho = 0, \; t > 0$),

$$\mathrm{D}_{S,m}\frac{\partial S_m}{\partial \rho}\Big|_{\rho=0} = 0, \quad \mathrm{D}_{P,m}\frac{\partial P_m}{\partial \rho}\Big|_{\rho=0} = 0. \tag{9}$$

2.3 Initial Conditions

Modeling batch type stirred tank reactors authors experiment planning vary a lot. The final case of experiment is clear reactions reach quazi-steady-state substrate concentration approach to zero and transient effectiveness factor approach to limiting values [11]. However, the time until the quazi-steady-state is reached, or amount of product is produced in fixed time vary a lot. The initial conditions in the bulk:

$$S_m(\rho, 0) = 0, \; P_m(\rho, 0) = 0, \; 0 < \rho < \rho_0 \tag{10}$$

$$S_b(\rho_1) = S_0, \; P_b(\rho) = 0, \tag{11}$$

which equivalence that no product appear in solution, there is no substrate in MR and the substrate concentration equal to initial concentration. Different initial conditions is respect to Nernst layer. First initial condition:

$$S_d(\rho, 0) = 0, \quad \rho_0 < \rho < \rho_1 \tag{IC1}$$

which equivalent to case when microreactors are injected in substrate, or substrate is filled on microreactors which are in neutral solution. The reaction starts, when solution difund to MR.

Second initial condition:

$$S_d(\rho, 0) = S_0, \quad \rho_0 < \rho < \rho_1, \tag{IC2}$$

which equivalent to case when microreactors in placed in MR, or substrate is pour on microreactors. In such case reaction starts immediately.

2.4 Microbioreactor Characteristics

The transient effectiveness factor η can be calculated [6,43],

$$\eta(t) = \frac{3(\mathrm{K_M} + S_b(t))}{S_b(t)\,\rho_0^3} \int_0^{\rho_0} \frac{S_m(\gamma, t)}{\mathrm{K_M} + S_m(\gamma, t)}\,\gamma^2\,\mathrm{d}\gamma. \tag{12}$$

Depending on the batch system configuration, the overall transient effectiveness factor can be equal, larger or smaller than the steady state effectiveness factor [12]. Analytical expressions of the steady state transient effectiveness factor (η_{ss}) effectiveness factors for the corresponding CSTR system have been recently derived [6],

$$\eta_{ss} = \frac{3\beta\phi(\sigma\coth\sigma - 1)}{\sigma^2(\beta + \phi(\sigma\coth\sigma - 1))}. \tag{13}$$

The expression (13) were derived for CSTR acting at low concentrations of the substrate when the Michaelis-Menten kinetics approaches the first-order kinetics. Since in BSTR, the substrate concentration in the bulk continuously decreases over time, these expressions of the steady state effectiveness factors are applicable also to BSTR independently from the initial concentration of the substrate [9,11,31].

The process duration is also among the most important characteristics of biotechnological processes [27]. A minimization of time-cost is often sought by designers of biotechnological processes [40]. The batch time required to achieve a certain conversion of the reactants is usually assumed as the main characteristic of the process duration [20]. The time $t_{0.5}$ and the corresponding dimensionless time $T_{0.5}$ required to convert a half of the initial amount of the substrate were used to investigate the process duration,

$$\begin{aligned} t_{0.5} &= \{t : S_b(t) = 0.5S_0\}, \\ T_{0.5} &= \{T : \widetilde{S}_b(T) = 0.5\widetilde{S}_0\}. \end{aligned} \tag{14}$$

The performance of the catalytic reactors is usually analysed in terms of the diffusion module, Biot number and inverse absorption capacity [2,35].

3 Dimensionless model

In order to define the main governing parameters of the two compartment model (3)-(IC2), the dimensional variable ρ and unknown concentrations

$S_m(\rho,\ t), P_m(\rho,\ t), S_d(\rho,\ t), P_d(\rho,\ t)$ are replaced with the following dimensionless parameters:

$$\begin{aligned}
&\widetilde{\rho} = \frac{\rho}{\rho_0},\ \ \widetilde{S}_m = \frac{S_m}{\mathrm{K_M}},\ \ T = \frac{\mathrm{D}_{S,m} t}{\rho_0^2},\ \ \theta = \frac{q}{\rho_0} \\
&\widetilde{P}_m = \frac{P_m}{\mathrm{K_M}},\ \ \widetilde{S}_d = \frac{S_d}{\mathrm{K_M}},\ \ \widetilde{P}_d = \frac{P_d}{\mathrm{K_M}}, \\
&\widetilde{\mathrm{D}}_{P,m} = \frac{\mathrm{D}_{P,m}}{\mathrm{D}_{S,m}},\ \ \widetilde{\mathrm{D}}_{S,d} = \frac{\mathrm{D}_{S,d}}{\mathrm{D}_{S,m}},\ \ \widetilde{\mathrm{D}}_{P,d} = \frac{\mathrm{D}_{P,d}}{\mathrm{D}_{S,m}},
\end{aligned} \tag{15}$$

where $\widetilde{\rho}$ is the dimensionless distance from the microreactor center and $\widetilde{S}_m(\widetilde{\rho},\ T), \widetilde{P}_m(\widetilde{\rho},\ T), \widetilde{S}_d(\widetilde{\rho},\ T), \widetilde{P}_d(\widetilde{\rho},\ T)$ are the dimensionless concentrations. Having defined dimensionless variables and unknowns, the following dimensionless parameters characterize the domain geometry and the substrate concentration in the bulk:

$$\widetilde{\nu}_1 = \frac{\nu}{\rho_0},\ \ \widetilde{S}_0 = \frac{S_0}{\mathrm{K_M}}, \tag{16}$$

where $\widetilde{\nu}_1$ is the dimensionless thickness of the Nernst diffusion layer, $\widetilde{\nu}_2 = \widetilde{\rho}_2 - \widetilde{\rho}_2$ is the dimensionless thickness of bulk, $\widetilde{S}_0$ is the dimensionless substrate concentration in the bulk solution. The dimensionless thickness of the microreactor equals one.

The governing equations (3) in the dimensionless coordinates are expressed as follows ($0 < \widetilde{\rho} < 1$):

$$\frac{\partial \widetilde{S}_m}{\partial T} = \frac{1}{\widetilde{\rho}^2}\frac{\partial}{\partial \widetilde{\rho}}\Big(\widetilde{\rho}^2 \frac{\partial \widetilde{S}_m}{\partial \widetilde{\rho}}\Big) - \sigma^2 \frac{\widetilde{S}_m}{1+\widetilde{S}_m}, \tag{17a}$$

$$\frac{\partial \widetilde{P}_m}{\partial T} = \widetilde{\mathrm{D}}_{P,m}\frac{1}{\widetilde{\rho}^2}\frac{\partial}{\partial \widetilde{\rho}}\Big(\widetilde{\rho}^2 \frac{\partial \widetilde{P}_m}{\partial \widetilde{\rho}}\Big) + \sigma^2 \frac{\widetilde{S}_m}{1+\widetilde{S}_m}, \tag{17b}$$

where σ is the Thiele modulus or the Damköhler number [24,38,42] defined as:

$$\sigma^2 = \frac{\mathrm{V_{max}}\rho_0^2}{\mathrm{K_M D}_{S,m}}. \tag{18}$$

The governing equations (4) take the following form ($1 < \widetilde{\rho} < 1 + \widetilde{\nu}$):

$$\frac{\partial \widetilde{S}_d}{\partial T} = \widetilde{\mathrm{D}}_{S,d}\frac{1}{\widetilde{\rho}^2}\frac{\partial}{\partial \widetilde{\rho}}\Big(\widetilde{\rho}^2 \frac{\partial \widetilde{S}_d}{\partial \widetilde{\rho}}\Big), \tag{19a}$$

$$\frac{\partial \widetilde{S}_d}{\partial T} = \widetilde{\mathrm{D}}_{P,d}\frac{1}{\widetilde{\rho}^2}\frac{\partial}{\partial \widetilde{\rho}}\Big(\widetilde{\rho}^2 \frac{\partial \widetilde{P}_d}{\partial \widetilde{\rho}}\Big). \tag{19b}$$

The matching conditions (7)-(IC2) become $T > 0$:

$$\frac{\partial \widetilde{S}_m}{\partial \widetilde{\rho}}\Big|_{\widetilde{\rho}=1} = \widetilde{\mathrm{D}}_{S,d}\frac{\partial \widetilde{S}_d}{\partial \widetilde{r}}\Big|_{\widetilde{\rho}=1} \tag{20a}$$

$$\frac{\partial \widetilde{P}_m}{\partial \widetilde{\rho}}\Big|_{\widetilde{\rho}=1} = \widetilde{\mathrm{D}}_{P,d}\frac{\partial \widetilde{P}_d}{\partial \widetilde{\rho}}\Big|_{\widetilde{\rho}=1}. \tag{20b}$$

$$\widetilde{S}_m(1) = \phi \widetilde{S}_d(1), \quad \widetilde{P}_m(1) = \phi \widetilde{P}_d(1). \tag{21}$$

$$\frac{\partial \widetilde{S}_m}{\partial \widetilde{\rho}}\Big|_{\widetilde{\rho}=0} = 0, \quad \frac{\partial \widetilde{P}_m}{\partial \widetilde{\rho}}\Big|_{\widetilde{\rho}=0} = 0, \tag{22a}$$

$$\widetilde{S}_d(\widetilde{\rho}, 0) = 0, \quad \widetilde{\rho}_0 < \widetilde{\rho} < \widetilde{\rho}_1 \tag{IC1D}$$

$$\widetilde{S}_d(\widetilde{\rho}, 0) = \widetilde{S}_0, \quad \widetilde{\rho}_0 < \widetilde{\rho} < \widetilde{\rho}_1 \tag{IC2D}$$

The dimensionless factor σ^2 essentially compares the rate of enzyme reaction ($V_{\max}/K_M$) with the diffusion through the enzyme-loaded microreactor ($D_{S,m}/\rho_0^2$). If $\sigma^2 \ll 1$, the enzyme kinetics controls the bioreactor action. The action is under diffusion control when $\sigma^2 \gg 1$.

The Biot number β is another dimensionless parameter widely used to indicate the internal mass transfer resistance to the external one [3,18],

$$\beta = \frac{\mathrm{D}_{S,d}\rho_0}{\mathrm{D}_{S,m}(\rho_1 - \rho_0)}. \tag{23}$$

When the Biot number is small, the effect of the external diffusion is the most marked. As the Biot number increases the effect of the external diffusion becomes less important. Typically, designers seek for bioreactors acting in the reaction-limited regime, since in this case reaction and diffusion occur on different time scales [23].

4 Numerical simulation of experiments

The nonlinear boundary value problem (3)-(11) was solved numerically, using the finite difference technique [22]. In the space direction ρ, the radius $[0, \rho_0]$ of the microreactor as well as the segment $[\rho_0, \rho_1]$ corresponding to the diffusion shell were divided into the same number N of subintervals. A uniform discrete grid was also introduced in the time direction t. An explicit finite difference scheme has been built as a result of the difference approximation [13]. $N = 120$ was constant in all the simulations, while the time step

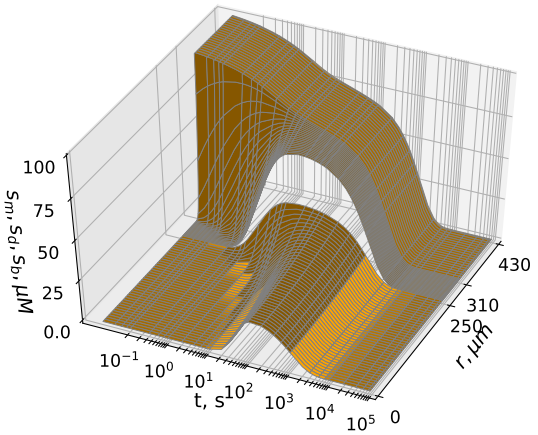

Figure 2: The dynamics of concentrations profiles S_m, S_d, S_b and transient effectiveness factor $\eta(t)$ with initial conditions (IC1).

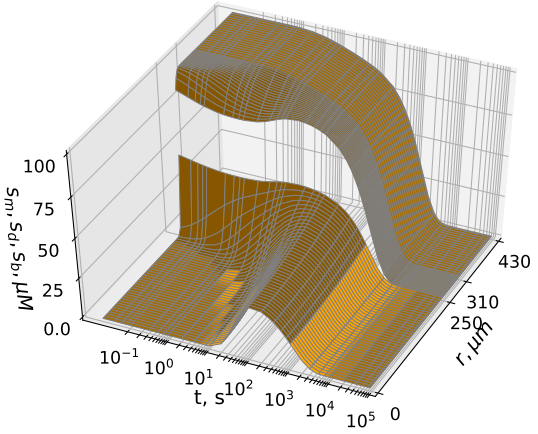

Figure 3: The dynamics of concentrations profiles S_m, S_d, S_b and transient effectiveness factor $\eta(t)$ with initial conditions (IC2).

size was recalculated for each simulation to make the difference scheme stable [13]. The simulator has been programmed by the authors in the C++ programming language [22]. The numerical solution of the problem (3)-(IC2) was validated by using known numerical solutions obtained for similar BSTR systems where the enzyme kinetics approaches the first-order kinetics and the external diffusion resistance is ignored [9, 10]. The solution was also compared with the exact analytical and approximate numerical solutions obtained for the corresponding CSTR system [6]. In all the numerical experiments, the following typical values of the model parameters were kept constant [19, 26]:

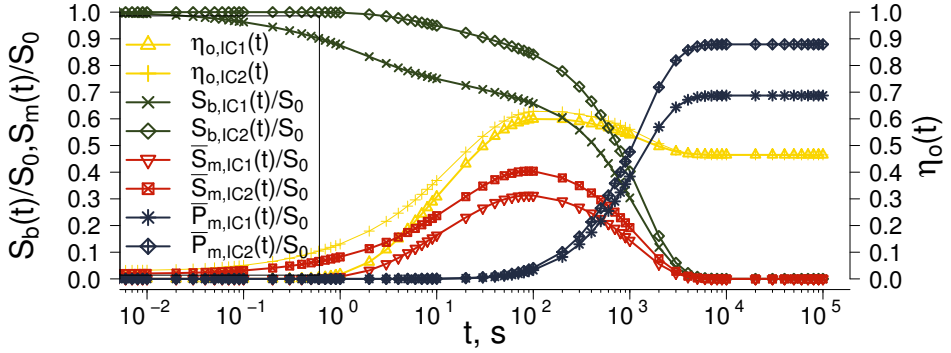

Figure 4: The dynamics of concentrations profiles $S_b(t), \bar{S}_m(t), \bar{P}_m(t)$ and transient effectiveness factor $\eta(t)$ for different initial conditions (IC1) and (IC2). The other parameters defined as in (24).

$$
\begin{aligned}
D_d = 600\,\mu\mathrm{m}^2/\mathrm{s},\ D_m = 200\,\mu\mathrm{m}^2/\mathrm{s},\\
K_M = 100\,\mu\mathrm{M},\ r_0 = 250\mu\mathrm{m},\ \phi = 0.6\\
V_{\max} = 1\,\mu\mathrm{M/s}, \rho_1 = 310\,\mu\mathrm{m}, \rho_2 = 430\mu\mathrm{m}
\end{aligned}
\tag{24}
$$

Figs. 2-3 shows the dynamics of the substrate concentration for the diffusion shell thickness ν_1 of $60\,\mu\mathrm{m}$, the convective shell thickness ν_2 of $120\,\mu\mathrm{m}$ and initial concentration $S_0 = K_M = 100\mu\mathrm{M}$ at different inital conditions (IC1) and (IC2), respectively. The dimensional parameters correspond to moderate values of the dimensionless parameters as follows: the diffusion module $\sigma \approx 1.77$, the Biot number $\beta = 15.5$, the ratio $\alpha = 3$, the inverse adsorption capacity $\theta \approx 0.7$ and the initial concentration $S_0 = 1$.

The kinetics of the substrate and product concentration in microreactor (Fig. 4) shows that the microbioreactor action finally approaches the steady state at zero substrate concentration in both, MR and bulk. As one can see in Fig. 4, the steady state transient effectiveness factors fit well with the effectiveness factor values calculated by formula (13): $\eta_{ss} = 0.487$.

The transient effectiveness factor reach maximums after approximately before the time when the average substrate concentration in the MR ($\bar{S}_m$) reaches its maximum ($t \approx 100\,\mathrm{s}$).

After this time elapsed, the microbioreactor system approaches a pseudo-equilibrium state, where both substrate concentrations, in bulk and averaged in the MR, do change but their relationship becomes constant [9].

It's worth to mention that product concentration reaches equilibrium state at different values. It's happens due different experiment planning. In condition IC1 the total amount is substrate is proportional to $4/3\pi\rho^3 - 4/3\pi\rho_1^3$, in case of IC2 the amount of substrate is proportional to $4/3\pi\rho^3 - 4/3\pi\rho_0^3$. So the final amount of product produced is proportional.

In order to investigate the different configurations of initial experiment, (17)-(22) was numerically simulated for different values of the dimensionless model parameters.

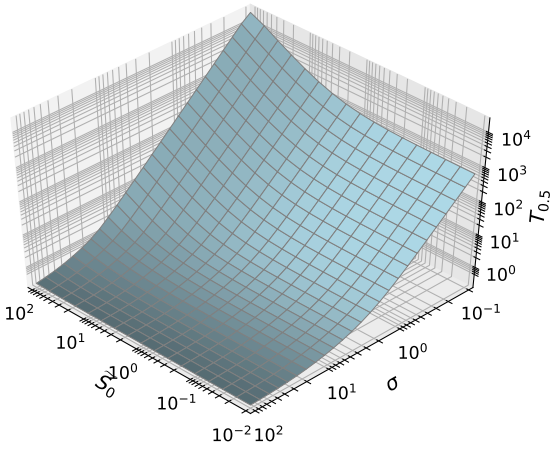

Figure 5: The dimensionless time $T_{0.5}$ vs. the diffusion module σ changing the initial concentration $\widetilde{S}_0$ at the ratio $\theta = 1$, $\beta = 10$ and init. condition (IC1).

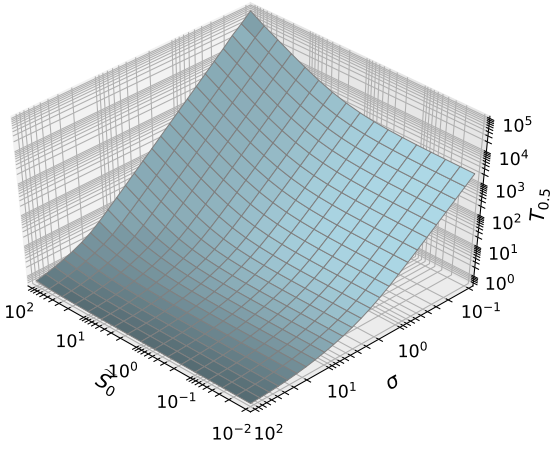

Figure 6: The dimensionless time $T_{0.5}$ vs. the diffusion module σ changing the initial concentration $\widetilde{S}_0$ at the ratio $\theta = 1$, $\beta = 10$ and init. condition (IC2).

4.1 Impact on process duration

To determine the influence of the diffusion limitations and the initial substrate concentration to the process duration, the MR action was simulated and the dimensionless holding time $T_{0.5}$ was calculated by changing values of the diffusion module σ, the Biot number β, the inverse absorption capacity θ and the dimensionless substrate concentration $\widetilde{S}_0$.

Figs. 5-6 shows the time $T_{0.5}$ versus the dimensionless concentration $\widetilde{S}_0$ and diffusion module σ at a mean value of the Biot number, $\beta = 10$. One can see in Figs. 5-6 a nonlinear increase in the time $T_{0.5}$ with increasing the substrate concentration $\widetilde{S}_0$. The time $T_{0.5}$ is particularly high at low values of the diffusion module σ, i.e. when the enzyme kinetics

controls the MR action. So, the increasing MR effectiveness by the decreasing internal diffusion limitation (decreasing σ) as well as by decreasing the substrate concentration is restricted when a short processing time is of crucial importance. The time difference at $\widetilde{S}_0 = 100, \sigma = 0.1$ is $T_{0.5,IC1} - T_{0.5,IC2} = 20000 - 90000 = -70000$.

Figs. 7-8 shows calculated values of the time $T_{0.5}$ versus $\widetilde{S}_0$ and β. As one can see in Fig. 7-8, the time $T_{0.5}$ increases with decreasing both, the initial concentration $\widetilde{S}_0$ and the Biot number β. The time difference at $\widetilde{S}_0 = 100, \beta = 100$ is $T_{0.5,IC1} - T_{0.5,IC2} = 225 - 912 = -687$.

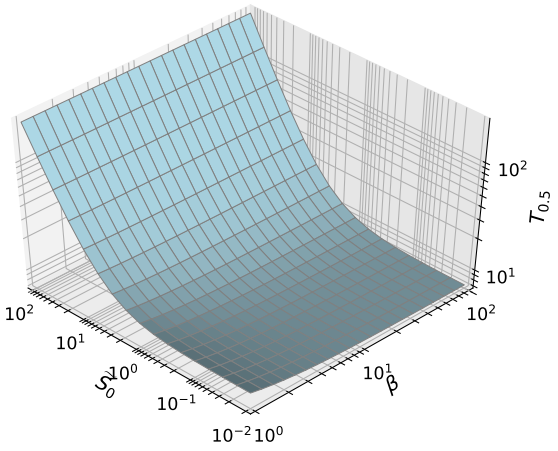

Figure 7: The dynamics of concentrations profiles $S_b(t)$ and transient effectiveness factor $\eta_o(t)$ for different initial conditions (IC1) and (IC2). (24).

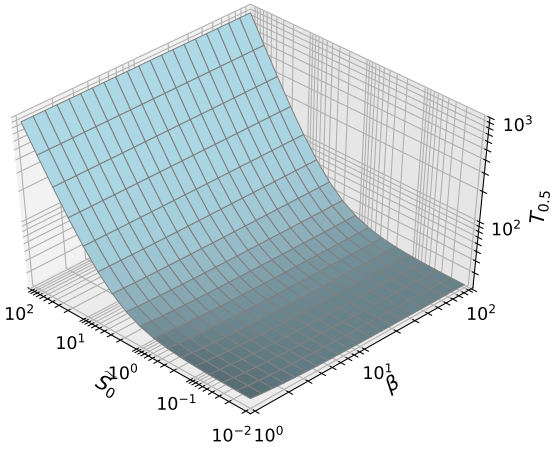

Figure 8: The dynamics of concentrations profiles $S_b(t)$ and transient effectiveness factor $\eta_o(t)$ for different initial conditions (IC1) and (IC2). (24).

Figs. 9-10 shows calculated values of the time $T_{0.5}$ versus $\widetilde{S}_0$ and θ. One can see in Figs. 9 - 10 a nonlinear increase in the time $T_{0.5}$ with increasing the inverse absorption capacity θ. The time $T_{0.5}$ is particularly high at low values of the inverse absorption capacity θ, i.e. when the microreactors are relatively small in comparison with bulk volume.

The break point is appear in using (IC1) condition, on changing inverse absorption capacity. The break point is around value $\theta \approx 0.7$ is related with process duration definition of half time $T_{0.5}$. In case (IC1) reaction in MR is not start until substrate difund to MR, since there is no substrate in Nernst layer. In this case half concentration is reached in S_b due fast difund to Nersnt layer see figure 2. The time difference at $\widetilde{S}_0 = 100, \theta = 10$ is $T_{0.5,IC1} - T_{0.5,IC2} = 5530 - 6932 = -1402$.

So, the decreasing the substrate concentration as well as increasing the number of particles (decreasing bulk volume) is restricted when a short processing time is of crucial importance.

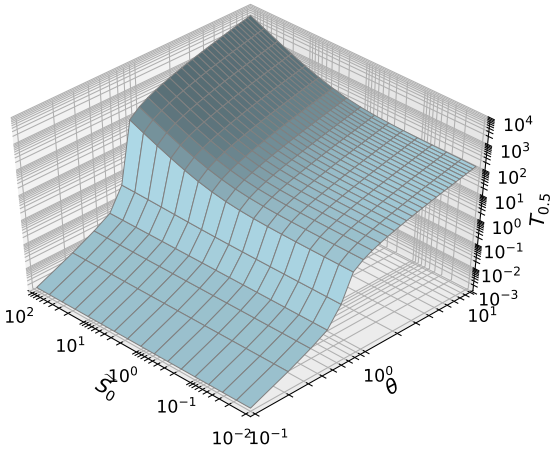

Figure 9: The dynamics of concentrations profiles $S_b(t)$ and transient effectiveness factor $\eta_o(t)$ for different initial conditions (IC1) and (IC2). (24).

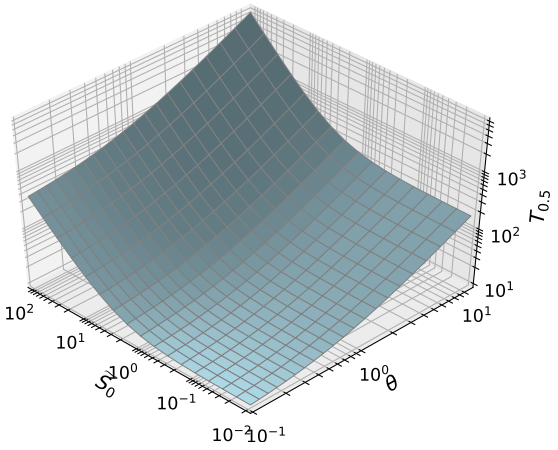

Figure 10: The dynamics of concentrations profiles $S_b(t)$ and transient effectiveness factor $\eta_o(t)$ for different initial conditions (IC1) and (IC2). (24).

5 Conclusions

The numerical simulation of different microreactors injections into batch stirred tank reactor was investigated. The two-compartment mathematical model 3-(IC1) and the corresponding dimensionless model (17)-(22) of a porous spherical microbioreactor acting in the batch flow can be successfully used to investigate the dependence of the internal and external diffusion limitations on the bioreactor process duration, as well as to optimize the MR configuration (Fig. 4).

The simulation showed significant time differences between microreactors injection vs. placing modes, in respect, the time is needed to achieve fixed amount of product quantity or substrate used until half-time Figs. (5-10).

Decreasing the MR substrate consumption time by increasing the internal diffusion limitation (increasing σ) as well as by decreasing the substrate concentration (S_0) and decreasing bulk volume (decreasing θ) is necessary when a short processing time is of crucial importance (Figs. 5-10).

These scientific modelling results will help to create microreactors more efficiently at the design stage.

References

[1] Otute Akiti and Piero M Armenante. Experimentally-validated micromixing-based cfd model for fed-batch stirred-tank reactors. *AIChE journal*, 50(3):566–577, 2004.

[2] Ali E. AL-Muftah and Ibrahim M. Abu-Reesh. Effects of simultaneous internal and external mass transfer and product inhibition on immobilized enzyme-catalyzed reactor. *Biochem. Eng. J.*, 27(2):167–178, 2005.

[3] Rutherford Aris. *Mathematical Modeling: a Chemical Engineer's Perspective*, volume 1. Academic Press, 1999.

[4] Romas Baronas, Feliksas Ivanauskas, and Juozas Kulys. *Mathematical Modeling of Biosensors*. Springer, Dordrecht, 2010.

[5] Romas Baronas, Juozas Kulys, and Linas Petkevičius. Computational modeling of batch stirred tank reactor based on spherical catalyst particles. *Journal of Mathematical Chemistry*, Sep 2018.

[6] Romas Baronas, Juozas Kulys, and Linas Petkevičius. Modelling the enzyme catalysed substrate conversion in a microbioreactor acting in continuous flow mode. *Nonlinear Anal. Model. Control*, 23(3):437–456, 2018.

[7] Philip N. Bartlett. *Bioelectrochemistry: Fundamentals, Experimental Techniques and Applications*. John Wiley & Sons, Chichester, UK, 2008.

[8] M Benítez, A Bermúdez, and JF Rodríguez-Calo. Adjoint method for parameter identification problems in models of stirred tank chemical reactors. *Chemical Engineering Research and Design*, 123:214–229, 2017.

[9] Claudia María Bidabehere, Juan Rafael García, and Ulises Sedran. Use of stirred batch reactors for the assessment of adsorption constants in porous solid catalysts with simultaneous diffusion and reaction. Theoretical analysis. *Chem. Eng. Sci.*, 61(6):2048–2055, 2006.

[10] Claudia María Bidabehere, Juan Rafael García, and Ulises Sedran. Transient effectiveness factor in porous catalyst particles. application to kinetic studies with batch reactors. *Chem. Eng. Res. Des.*, 118:41–50, 2017.

[11] Claudia María Bidabehere, Juan Rafael García, and Ulises Sedran. Transient effectiveness factor. simultaneous determination of kinetic, diffusion and adsorption equilibrium parameters in porous catalyst particles under diffusion control conditions. *Chemical Engineering Journal*, 345:196–208, 2018.

[12] Claudia María Bidabehere and Ulises Sedran. Transient effectiveness factors in the dynamic analysis of heterogeneous reactors with porous catalyst particles. *Chem. Eng. Sci.*, 137:293–300, 2015.

[13] Dieter Britz and others. *Digital Simulation in Electrochemistry*, volume 666. Springer, 2005.

[14] Dieter Britz and Jörg Strutwolf. *Digital Simulation in Electrochemistry*. Monographs in Electrochemistry. Springer, 4 edition, 2016.

[15] Dan Caşcaval, Alexandra Cristina Blaga, and Anca-Irina Galaction. Diffusional effects on anaerobic biodegradation of pyridine in a stationary basket bioreactor with immobilized Bacillus spp. cells. *Environmental Technology*, pages 1–13, 2017.

[16] M. F. Chaplin and C. Bucke. The large-scale use of enzymes in solution. *Enzyme Technology*, pages 138–166, 1990.

[17] Margarita Andreas Dareioti and Michael Kornaros. Effect of hydraulic retention time (HRT) on the anaerobic co-digestion of agro-industrial wastes in a two-stage CSTR system. *Bioresource Technology*, 167:407–415, 2014.

[18] Mark E. Davis and Robert J. Davis. *Fundamentals of Chemical Reaction Engineering*. MGraw-Hill, New York, 2003.

[19] Duong D. Do and Paul F. Greenfield. The concept of an effectiveness factor for reaction problems involving catalyst deactivation. *Chem. Eng. J.*, 27(2):99–105, 1983.

[20] Pauline M. Doran. *Bioprocess Engineering Principles*. Academic Press, 1995.

[21] Suresh Kumar Dubey, Ashok Pandey, and Rajender Singh Sangwan. *Current Developments in Biotechnology and Bioengineering: Crop Modification, Nutrition, and Food Production*. Elsevier, 2016.

[22] Daniel J Duffy. *Finite Difference methods in financial engineering: a Partial Differential Equation approach*. John Wiley & Sons, 2013.

[23] D. A. Edwards, B. Goldstein, and D. S. Cohen. Transport effects on surface-volume biological reactions. *Journal of Mathematical Biology*, 39(6):533–561, 1999.

[24] David J. Fink, Tsungyen Na, and Jerome S. Schultz. Effectiveness factor calculations for immobilized enzyme catalysts. *Biotechnology and Bioengineering*, 15(5):879–888, 1973.

[25] H. Gutfreund. *Kinetics for the Life Sciences*. Cambridge University Press, Cambridge, 1995.

[26] Andrés Illanes. *Enzyme biocatalysis: principles and applications*. Springer Science & Business Media, 2008.

[27] Jamshed Iqbal, Shoaib Iqbala, and Christa E. Müller. Advances in immobilized enzyme microbioreactors in capillary electrophoresis. *Analyst*, 138(11):3104–3116, 2013.

[28] Rohan Karande, Andreas Schmid, and Katja Buehler. Applications of multiphasic microreactors for biocatalytic reactions. *Organic Process Research & Development*, 20(2):361–370, 2016.

[29] Matthew B. Kerby, Robert S. Legge, and Anubhav Tripathi. Measurements of kinetic parameters in a microfluidic reactor. *Analytical Chemistry*, 78(24):8273–8280, 2006.

[30] Aikaterini Konti, Diomi Mamma, Dimitios G. Hatzinikolaou, and Dimitris Kekos. 3-Chloro-1, 2-propanediol biodegradation by Ca-alginate immobilized Pseudomonas putida DSM 437 cells applying different processes: mass transfer effects. *Bioprocess and Biosystems Engineering*, 39(10):1597–1609, 2016.

[31] G. Marroquín, J. Ancheyta, and C. Esteban. A batch reactor study to determine effectiveness factors of commercial HDS catalyst. *Catal.Today*, 104(1):70–75, 2005.

[32] Atsuko Miyawaki, Shunya Taira, and Fumihide Shiraishi. Performance of continuous stirred-tank reactors connected in series as a photocatalytic reactor system. *Chemical Engineering Journal*, 286:594–601, 2016.

[33] MA Noriega, PC Narváez, JG Cadavid, and AC Habert. Modeling of biodiesel production in liquid-liquid film reactors including mass transfer effects. *Fuel Processing Technology*, 167:524–534, 2017.

[34] Félix Monteiro Pereira and Samuel Conceição Oliveira. Occurrence of dead core in catalytic particles containing immobilized enzymes: analysis for the michaelis–menten kinetics and assessment of numerical methods. *Bioprocess and Biosystems Engineering*, 39(11):1717–1727, 2016.

[35] L Petkevičius and Romas Baronas. Numerical simulation and analysis of enzyme-catalysed substrate conversion in a microbioreactor. In *SIMUL 2017: The Ninth International Conference on Advances in System Simulation*, pages 8–12, 2017.

[36] Linas Petkevicius and Romas Baronas. Modeling and simulation of enzyme-catalysed substrate conversion in a microbioreactor. *International Journal on Advances in Systems and Measurements*, 11(1-2):173–182.

[37] Harshada M Salvi, Manoj P Kamble, and Ganapati D Yadav. Synthesis of geraniol esters in a continuous-flow packed-bed reactor of immobilized lipase: Optimization of process parameters and kinetic modeling. *Applied biochemistry and biotechnology*, 184(2):630–643, 2018.

[38] Th Schulmeister. Mathematical modelling of the dynamic behaviour of amperometric enzyme electrodes. *Selective Electrode Reviews*, 12(2):203–260, 1990.

[39] Lee A. Segel and Marshall Slemrod. The quasi-steady-state assumption: a case study in perturbation. *SIAM Review*, 31(3):446–477, 1989.

[40] T Skybová, M Přibyl, and P Hasal. Mathematical model of decolourization in a rotating disc reactor. *Biochemical Engineering Journal*, 93:151–165, 2015.

[41] Momchil Velkovsky, Rachel Snider, David E. Cliffel, and John P. Wikswo. Modeling the measurements of cellular fluxes in microbioreactor devices using thin enzyme electrodes. *Journal of Mathematical Chemistry*, 49(1):251–275, 2011.

[42] John Villadsen, Jens Nielsen, and Gunnar Liden. *Bioreaction Engineering Principles*. Springer, Dordrecht, 2011.

[43] H. J. Vos, P. J. Heederik, J. J. M. Potters, and K. Ch. A. M. Luyben. Effectiveness factor for spherical biofilm catalysts. *Bioprocess Eng.*, 5(2):63–72, 1990.

[44] Joseph Wang. *Analytical Electrochemistry*. John Wiley & Sons, Joboken, New Jersey, 3 edition, 2006.

[45] Jonathan WC Wong, R. D. Tyagi, and Ashok Pandey. *Current Developments in Biotechnology and Bioengineering: Solid Waste Management*. Elsevier, 2016.